JOURNAL OF GEOPHYSICAL RESEARCH, VOL. 111, D24302, doi:10.1029/2006JD007144, 2006

Formation, transformation, and removal of aerosol over a tropical mangrove forest

A. Chatterjee,[1] C. Dutta,[1] S. Sen,[1] K. Ghosh,[2] N. Biswas,[2] D. Ganguly,[3] and T. K. Jana[3]

Received 1 February 2006; revised 7 July 2006; accepted 10 August 2006; published 19 December 2006.

[1] A comprehensive size-segregated characterization of the chemical properties (water-soluble inorganic fraction) of the sea-salt aerosol originated from the surf zone at the land-ocean boundary of Sundarban Mangrove forest, NE coast of Bay of Bengal, and an analysis of the relevant meteorological parameters revealed how the combined effect of anthropogenic gases and aerosol advected to the virgin mangrove forest and micrometeorological conditions could change the marine character of the aerosol before the onset of SW monsoon. The average aerosol mass concentration was 99.94 ± 41.9 $\mu g\ m^{-3}$ with production rate of 0.19 $\mu g\ m^{-2}\ s^{-1}$ (during January) to 4.29 $\mu g\ m^{-2}\ s^{-1}$ (during April) and dry deposition rate of 0.019 $\mu g\ m^{-2}\ s^{-1}$ (during January) to 13.21 $\mu g\ m^{-2}\ s^{-1}$ (during June). 72.35% of the total aerosol mass was leachable by water, and relatively large concentrations of phosphorus were observed. More chloride depletion from the coarse ($2.0 < d_p < 10$ μm) and nucleation ($d_p < 0.4$ μm) modes compared to the accumulation mode ($0.4 < d_p < 2.0$ μm) was observed in winter (Cl/Na = 0.6023 ± 0.1798), and a reverse trend was observed in summer (Cl/Na = 0.644 ± 0.262). A significant positive correlation was obtained for chloride loss with non-sea-sulphate and nitrate for particles > 2.0 μm. Distributions of Na^+, K^+, Ca^{2+}, Mg^{2+}, NH_4^+, Cl^-, NO_2^-, NO_3^-, SO_4^{2-}, and PO_4^{3-} in different size modes were considered to collate their source apportionment. The proximity of Calcutta and Haldia metropolis to the mangrove forest could influence the forest air quality and depositional processes.

Citation: Chatterjee, A., C. Dutta, S. Sen, K. Ghosh, N. Biswas, D. Ganguly, and T. K. Jana (2006), Formation, transformation, and removal of aerosol over a tropical mangrove forest, *J. Geophys. Res.*, *111*, D24302, doi:10.1029/2006JD007144.

1. Introduction

[2] Mangrove forests belong to the major ecosystems of the biosphere, and about 60 to 75% of tropical coasts are fringed by this highly productive ecosystem [*Clough*, 1998]. In the tropics and subtropics, mangroves cover 100,000–230,000 km^2 and are the major ecosystems fringing the continental margins. Because of their high productivity and turnover rates of the organic matter and exchange of materials from this biosphere with atmosphere, terrestrial and marine ecosystems, mangroves are of particular importance for the biogeochemical cycling of carbon and associated elements along with the continental margins [*Clough*, 1998]. The mangrove systems are the ecosystems at the land-sea margin whose area has been largely reduced in the past decades because of man's activities [*Jennerjahn and Ittekkot*, 2002]. Growing populations and associated increased emissions to the atmosphere and water together with fast land use changes, the coastal ocean atmospheric systems represent a complicated and stressed chemical environment that can have the global implication for climate [*Raes et al.*, 2000]. Concentration of homogenous hetero molecular nucleation of natural atmospheric aerosol close to the shoreline rises from background level during clean marine airflow. Nucleation appears to be a frequent phenomenon in the continental boundary layer and evidence of new particle formation has been reported for environments like coastal areas of North Atlantic in relation to tidal cycle [*O'Dowd et al.*, 1998] and for highly polluted industrialized agricultural regions of Germany and Italy [*Birmili and Wiedensohler*, 2000; *Laaksonen et al.*, 2005]. The land-ocean boundary of the Sundarban Mangrove forest, NE coast of the Bay of Bengal is highly irregular and criss-crossed by the several rivers and waterways. East to west this area is about 140 km from the east boundary to the west boundary and 50–70 km from the shore line to the north boundary. Several discrete islands and low-lying intertidal zone is covered with thick mangrove forest. The intertwining roots of the plants in the littoral zone breaks the wind induced waves and reduces the water velocities. This results the production of sea salt aerosol from the bursting of air-entrained bubbles during the breaking of waves. Contribution of the wind-blown excreted salts from various halophytic plants genera such as *Avicennia, Accanthus, Aegiceras, Bruguiera*, and *Ceriops* etc. could be significant for aerosol formation. Height of the natural mangrove plants greater than 10 m is rare. The climate of this area is

[1]Department of Chemistry, Calcutta University, Calcutta, India.
[2]Glass Physics Section, Central Glass and Ceramic Research Institute, Jadavpur, Calcutta, India.
[3]Department of Marine Science, Calcutta University, Calcutta, India.

0148-0227/06/2006JD007144

dominated by Southwest monsoon (June–September) and Northeast monsoon (October–January). The seasonal movement of Inter Tropical Convergence Zone during NE monsoon could cause the polluted continental air to overlap with the virgin mangrove forest environment. This globally important ecosystem is characterized by exchange of both aerosol promoting and nonpromoting biogenic gases [*Mukhopadhyay et al.*, 2002; *Biswas et al.*, 2005]. This typical mangrove forest could result in rapid vertical mixing of biogenic gases and aerosols to high altitude, where they can be transported over long distance affecting tropospheric chemistry. Several studies involving aerosol production and chemical composition measurements have been reported in tropical rain forest [*Artaxo et al.*, 1990, 1994, 1998]. Despite the important role played by the mangroves in the biogeochemical cycle of the coastal as well as offshore environment, very few quantitative studies have been carried out in the past to clarify the extent to which mangrove represent a significant source of aerosol.

[3] Considering the close proximity of this ecosystem to the metropolis and industrial town like Calcutta and Haldia mass loading and dry deposition of sea-salt aerosol at the land ocean boundary condition of this coastal Sundarban mangrove environment was studied along with its size-segregated chemical composition, distribution and quantitative source apportionment during Asian dry season between November and June with the objective of assessing the impact of anthropogenic gases and aerosol advected to the measurement site.

2. Sampling Location

[4] The area of Indian Sundarban Mangrove forest is 9630 km^2 out of which 4264 km^2 is under reserve forest in the estuarine phase of the river Ganges (Figure 1). It is a unique bioclimatic zone at land-ocean boundary of Bay of Bengal (20°32′–20°40′N and 88°05′–89°E) and the largest delta on the globe. Several discrete islands constitute Sundarban. The largest island in the row, Sagar Island, covering an area of 300 km^2, is situated at the confluence of Hooghly River and Bay of Bengal. Human activities as well as changes in the land use through reclamation for the agriculture and aquaculture have altered natural mangrove vegetation cover at this island. Lothian Island covering an area of 38 km^2, has been notified as a sanctuary and is situated at the confluences of Saptamukhi River and Bay of Bengal.

[5] Measurements were carried out at two stations: one located at Sagar Island (Seamapore tower situated at a distance of 250 m from the shore line) and the other one at Lothian Island located at a distance of about 40 km from the Seamapore tower. Both the towers were about 20 m high and the aerosol sampler was employed on a platform at 10 m height of the tower.

3. Experimental Method

[6] Sampling period of aerosol was from November 2004 – June 2005 and a total of five sets of samples were collected. Each event began at 0600 LT. and lasted for about 40 hours. Sampling was done at both the stations one immediately after another. The sampling schedule and meteorological parameters are detailed in Table 1 (all times are local time). Size-segregated aerosol samples were collected using a battery operated cascade impactor (flow rate 1.7 $m^3\ h^{-1}$) fitted with a pre separator (Pacwill Environmental, Canada) and particles were classified into nine size fractions according to the following equivalent aerodynamic cut off diameters: 0.4;0.7;1.1;2.1;3.3;4.7;5.8;9;10 μm. On the quartz fiber substrate (diameter 81mm, ashed at 700°C for 24 hours and carefully equilibrated in desiccators) total aerosol mass was measured by weighing the substrate, before and after sampling using a microbalance (Metler AE 240) in a controlled environment chamber maintained at a temperature of 23 ± 2°C and relative humidity of 35 ± 5%. The temperature, humidity, pressure, wind speed and its direction, were simultaneously recorded at two different heights (10 m and 15 m) by a computerized weather station (Model: Davis 7440), using different probes. Measurements of the micrometeorological parameters were done only during the limited hours of aerosol collections. The planetary boundary layer (PBL) height (h) was estimated [*Pal Arya*, 2001] using the relation: $h = 0.25u_*/|F|$ and u_* (frictional velocity) was calculated from wind velocity (u) at two different heights, z_1 and z_2 using the relation $u_* = k\{uz_2 - uz_1\}/\ln(z_2/z_1)$, where k = Von Karman constant (0.4) and F = Coriolis parameter related to the rotational speed of the earth (Ω) and latitude as $F = 2\Omega \sin \varphi$.

[7] Water-soluble inorganic species like Na^+, NH_4^+, K^+, Ca^{2+}, Mg^{2+}, Cl^-, NO_2^-, NO_3^-, PO_4^{3-} and SO_4^{2-} at each stage were extracted by ultrasonic agitation using 20 ml deionized water for 20 minutes using a procedure similar to those described by *Zhuang et al.* [1999]. The extracts were filtered through nylon membrane filter paper and kept in the prewashed polypropylene bottles. Chemical analysis for the water soluble inorganic ions were conducted by Ion Chromatography (Metrohm 792 basic IC) using separator columns, (Metrosep cation 1–2 (6.1010.000)) for cation and (Metrosep A Supp 3 (6.1005.320)) for anion analysis, fitted with a guard column (PRP-1 IC guard column cartridge (6.1005.050)). The eluents were a mixture of 1.8 mmol L^{-1} Na_2CO_3 and 1.7 mmol L^{-1} $NaHCO_3$ for anion and a mixture of 0.75 mmol L^{-1} pyridine dicarboxylic acid and 4 mmol L^{-1} L (+) tartaric acid for cation analysis and were passed at a flow rate of 1 ml min^{-1}. The detection limits were 0.008 $\mu g\ m^{-3}$ for SO_4^{2-}, Cl^-, and NH_4^+, 0.005 $\mu g\ m^{-3}$ for NO_3^-, NO_2^-, PO_4^{3-} and Mg^{2+} and 0.014 $\mu g\ m^{-3}$ for Na^+, and 0.011 $\mu g\ m^{-3}$ for Ca^{2+}.

[8] Salinity of the coastal water was determined by Mohr-Knudsen titration method. Standard seawater of chlorinity 19.374 procured from the National Institute of Oceanography, Goa, was used for standardization ($S = 1.80655 \times Cl$). Phosphate, nitrate, nitrite, ammonia were analyzed by spectrophotometric method [*Grasshoff et al.*, 1983]. NO_2 in ambient air was absorbed in 25 ml of sodium hydroxide in sodium arsenate solution and concentration of NO_2 in the mixture was estimated by spectrophotometric method [*Jacobs and Hochhieser*, 1958]. NH_3 was absorbed in 10 ml 0.1N H_2SO_4 and after mixing with phosphate buffer determined spectrophotometrically by indophenol blue method [*APHA*, 1977].

[9] For estimating the aerosol flux, a distributed area source is considered in which the offshore and nearshore area contributions is treated as coming from a continuous

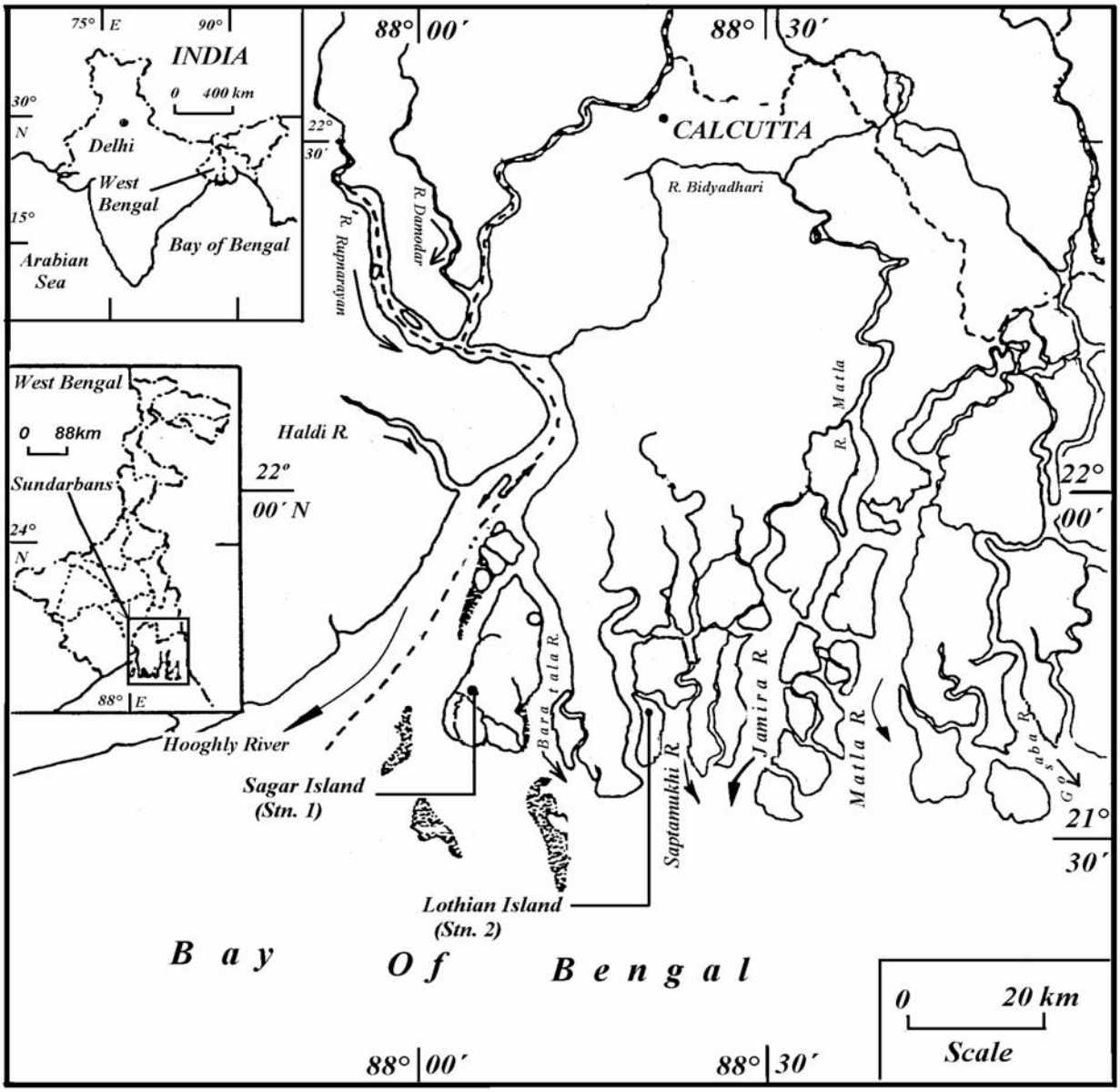

Figure 1. Map showing the station location.

distribution of infinitesimal sources. Aerosol occurs neither as point sources (for whitecaps) nor as line sources (for surf zone) from an atmospheric diffusion viewpoint. Considering the emissions of aerosol from an area at a uniform rate of F gm $m^{-2}s^{-1}$ with an atmospheric concentration of χ μg m^{-3} and average wind speed of u m s^{-1} over the phase distance X from a receptor point to the upwind edge of the sea source, the following equation [*Gifford and Hanna*, 1973] was used for flux calculation:

$$F = \chi u/C,$$

where $C = 0.7979\ X/\sigma z\ (1 - b)$ and $\sigma z = aX^b$.

[10] Values of a and b for different atmospheric dispersion conditions are compared according to *Pasquill and Smith* [1983]. The generation of aerosol depends on the phase distance, which govern the sea state and whitecaps distributions and subaqueous bathymetry, which controls the breaking wave condition in the surf zone apart from wind speed, direction and duration in the coastal area. Whitecaps were observable with an upwind distance of 50 meter. *Hsu and Whelan* [1976] examined the validity of the *Gifford and Hanna* [1973] model to a surf zone and the predicted data were found in good agreement with those obtained on open coasts in Texas and Hawaii and a protected coast on Barbados [*Duce and Woodcock*, 1971; *Hoffman and Duce*, 1972]. The aerosol flux values reported here are to be considered as estimates rather than absolute values.

[11] Dry deposition fluxes (F_d) of different size fractions were determined using the dry deposition velocity model developed by *Sehmel and Hodgson* [1978]. This model divides the mass size distribution into a number of intervals with different deposition velocity and the calculated dry

Table 1. Sampling Schedule With Meteorological Conditions and Physicochemical Properties (Mean ± SD) of Coastal Water[a]

	22–26 Nov 2004	21–24 Jan 2005	1–4 March 2005	30 April to 3 May 2005	3–6 Jun 2005
Temperature, °C					
10 m	22.9 ± 3.47	17.98 ± 3.92	22.34 ± 3.04	30.2 ± 1.94	29.2 ± 2.35
15 m	22.5 ± 3.67	18.2 ± 4.37	27.90 ± 3.62	29.7 ± 1.57	28.57 ± 1.47
Wind Speed, m s^{-1}					
10 m	0.36 ± 0.38	0.46 ± 0.31	1.01 ± 0.91	5.74 ± 3.02	4.71 ± 0.9
15 m	0.9 ± 0.82	0.75 ± 0.47	2.33 ± 1.48	8.01 ± 3.34	7.05 ± 1.21
Wind direction, Degrees					
Night	270–315	315–360	315–360	135–270	135–270
Day	225–270	0–45	0–45		
RH, %	76.8 ± 14.6	75.13 ± 14.09	74.13 ± 14.57	76.2 ± 7.27	91.46 ± 3.73
Pressure, mm	760.7–764	763–768.3	759.1–762.6	753–758	754.3–757
PBL, m	2545	1324	4018	1871	1948
u_*, ms^{-1}	0.5	0.29	1.3	2.24	2.31
z_0, m	7.65	5.27	7.33	3.58	4.39
Salinity, %	15.72	23.1	25.81	25.9	19.43
PO_4^{3-}–P, μM	1.32	0.69	1.81	2.77	1.7
NO_3^-–N, μM	10.62	10.22	18.87	14.15	16.3
NH_4^+–N, μM	0.97	0.73	0.72	0.15	0.21

[a]RH is relative humidity; PBL is planetary boundary layer; u* is frictional velocity.

deposition flux for each interval is then summed to calculate the total flux.

[12] $F_d = \Sigma CiV_d$, where Ci = concentration of different size fraction measured by each impactor stage and Vd = deposition velocity of the particle for each impactor stage and is calculated using the relation:

[13] V_d (cm s^{-1}) = exp {7.1108 + [ln (Sc)ln (d/z_0)] [0.02529 − 0.00273 ln (d/z_0)] + [ln (Υ^+)] [0.03239 ln (Υ^+) − 0.09177 ln (d/z_0)] − 0.14919 [ln(d)]^2 − 4.180 ln (d/z_0) where: d = particle diameter (cm), Sc = Schmidt number (ν/D), u_* = friction velocity (cm s^{-1}), z_0 = aerodynamic surface roughness (cm), ν = kinematic viscosity (μ/ρ), ρ = air density (g cm^{-3}), D = Brownian diffusion coefficient (cm^2 s^{-1}), Υ^+ = dimension less relaxation time [$(\rho_P\ d^2\ u_*^2/(18\mu\nu)$], ρ_P = particle density, (g cm^{-3}), μ = air viscosity (g cm^{-1} s^{-1}). This model has been used previously and produced the best calculated/measured flux ratio (1:1) and smallest standard deviation (±0.42) [*Lin et al.*, 1993; *Lestari et al.*, 2003]. Values of viscosity of the air at the observed temperature and pressure and densities of the aerosol particles were adopted as given by *Williamson* [1973].

[14] The relative random uncertainties of the main aerosol component concentration for each impactor stage were obtained, using the procedure of error propagation described by *Putaud et al.* [2000], and including (1) uncertainty in the sampled air volume, ±3%, (2) weighing precision ±2 μg, (3) precision of the extraction water volume, ±0.05 ml, (4) the relative error in ion chromatographic measurements, −1.95 to +2.33%, and (5) blank variability ±49.6, ±14.5, ±5.5, ±14.17, ±16.92, ±4.16 μg L^{-1} for Na^+, Cl^-, NH_4^+, NO_3^-, SO_4^{2-}, and PO_4^{3-}, respectively. Before running water extract of the sample in the ion chromatograph simulated rainwater standard reference material from National Institute of Science and Technology, SRM No. 2694 – A was analyzed to estimate the relative error of individual ions.

4. Result and Discussion

[15] Temperature, wind speed and direction, Planetary Boundary Layer (PBL) given in Table 1 show lower values during the initial phase of the dry season (postmonsoon) compared to those observed during the last phase (premonsoon). However, relative humidity (RH) gradually decreases to a minimum value in March and again it increases to maximum value before the onset of monsoon. The average mass of total aerosol along with the concentration of major water soluble inorganic ions (Na^+, K^+, NH_4^+, Ca^{2+}, Mg^{2+}, Cl^-, NO_2^-, NO_3^-, PO_4^{3-}, SO_4^{2-}) are divided into three modes [*Pueschel*, 1995]: coarse ($2.0 < dp < 10\mu$m), accumulation ($0.4 < dp < 2.0\ \mu$m) and nucleation ($dp < 0.4\ \mu$m) and their size distributions are presented in Table 2. The average mass of aerosol (sum of all sizes) is 99.94 ± 41.9 μg m^{-3}. *Ganguly et al.* [2005] reported the surface level aerosol mass concentration of 100 μg m^{-3} over the Bay of Bengal during 19–28 February 2003. Over the Amazon forest, *Artaxo et al.* [1998] observed the average aerosol mass concentration of 107 ± 61 μg m^{-3} with a maximum value of 297 μg m^{-3} during biomass burning in the Amazon Basin. *Parameswaran et al.* [1999] estimated the mass loading of 20–130 μg m^{-3} aerosol over the Indian Ocean near to the Thiruvananthapuram coast. Figure 2 shows the variations of aerosol mass concentrations in different size during the study period. Its concentration showed a progressive decrease from 128.21 μg m^{-3} in November to a minimum value of 44.14 μg m^{-3} in March and again increased back

Table 2. Concentrations (Mean ± SD) of Water-Soluble Ions in Different Size Modes

Species	Coarse, μg m^{-3}	Accumulation, μg m^{-3}	Nucleation, μg m^{-3}
Total aerosol	56.99 ± 23.67	36.67 ± 14.98	6.42 ± 4.82
Na	13.41 ± 7.9	5.91 ± 5.19	1.49 ± 1.77
NH_4	0.11 ± 0.08	0.94 ± 0.91	0.38 ± 0.44
K	2.17 ± 1.37	0.54 ± 0.87	0.11 ± 0.21
Ca	2.95 ± 1.75	1.06 ± 1.01	0.33 ± 0.47
Mg	0.95 ± 1.42	0.50 ± 0.97	0.12 ± 0.23
Cl	7.92 ± 4.26	1.95 ± 1.37	0.61 ± 0.55
NO_2	0.08 ± 0.06	0.07 ± 0.1	0.04 ± 0.06
NO_3	1.55 ± 1.13	1.52 ± 1.61	0.66 ± 1.13
PO_4	7.07 ± 2.97	3.84 ± 0.94	0.9 ± 0.67
SO_4	7.02 ± 10.08	5.73 ± 6.42	1.33 ± 2.05
nss-SO_4	3.64	4.24	0.96

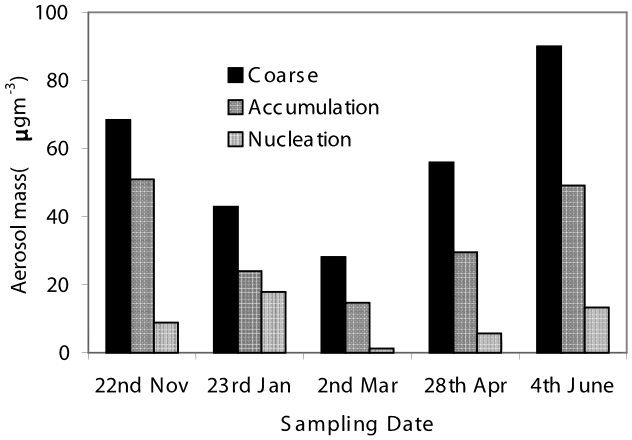

Figure 2. Datewise concentration of coarse, accumulation, and nucleation mode aerosol (average of two stations' data).

to 152.6 μg m^{-3} in June. *Rajeev et al.* [2004] also observed the larger aerosol optical depth (AOD) over the Arabian Sea and Bay of Bengal during February–April compared to that during November–January. Sea-salt aerosol loading over the surf zone before the onset of monsoon (April–June) was about 10 fold higher in magnitude (Figure 3) than that the rate observed during November–March. Lower rate of aerosol loading during March together with maximum PBL height of 4018 m could result less abundance of total aerosol in the atmosphere. Reversal of wind direction along with the decreased PBL height (Table 1) was a preindication of the onset of southwest monsoon. This resulted in the higher rate of loading of aerosol and its subsequent transport toward the continent. During the winter period (November–March) persistent north easterly flow with wind velocity between 0.75 and 2.33 m s^{-1} at 15 m and high pressure (759.1–768.3 mm) to the north of the equator gave rise to the PBL heights variation between 1324 and 4018 m with gradual decrease of temperature, humidity and aerosol concentration (128.2–44.14 μg m^{-3}). The seasonal movement of the Intertropical Convergence Zone (ITCZ) toward North during summer (April–June) prevailing southwesterly wind with 4.71–5.74 m s^{-1} velocity and low pressure (753–758 mm) caused variation of PBL heights between 1871 and 1948 m accompanying with increasing temperature, humidity and aerosol concentration (91.23–152.6 μg m^{-3}) in the atmosphere.

[16] Deposition velocity showed a wide range of variation with a minimum value of 0.02 cm s^{-1} in January and a maximum value of 7.6 cm s^{-1} in June. The decrease of deposition velocity with decreasing wind velocity also agrees with other literature data [*McDonald et al.*, 1982; *Petelski and Chomka*, 2000] The equation did not yield negative values of deposition velocity (V_d) for wind velocity between 0.36 and 5.74 m s^{-1}. Dry deposition rates varied between 0.019 and 13.21 μg m^{-2}s^{-1} with a maximum rate in June; which could be due to greater turbulent deposition as evident by the friction velocity, u_* of 2.31 m s^{-1}. A surf zone spans 140 km along the NE coast of Bay of Bengal and within an upwind distance of 50m from the shoreline was considered. The estimated width of the surf zone was 100m, which was on the higher end values observed by *De Leeuw et al.* [2000]. In this littoral region, wave breaking is dominated by interaction with the shallow sea bottom surface and low-lying islands covered with the thick mangrove forest. Extensive near complete whitecap coverage can develop even at very low wind speed. Integrating over the months with dry deposition of aerosol, the surf zone from receptor point to the upwind edge of the sea source (7×10^6 m^2) total amount of dry deposition was estimated to be 591 Mg with 34.7% sea salt aerosol contribution from surf zone and the rest being advected horizontally. Figures 4a and 4b represents the size distribution of aerosol flux for the month of November and March, respectively; which showed quadrimodal distribution with prominent peaks of lower intensity in the nucleation and accumulation modes compared to that of coarse mode. Table 2 shows the average aerosol concentration along with its water-soluble components in coarse, accumulation and nucleation mode. Water-soluble inorganic fraction accounts for 72.35% of the total aerosol mass. The rest of the mass could be due to water insoluble trace elements, black/organic carbon, water and the other components. During postmonsoon (November–January), the dominant wind direction was from North West to North East and contribution of accumulation mode was found to be increased from 39.7 to 46.0% indicating the effect of air borne mass from urban plume of Calcutta and Haldia metropolis reaching the sampling site. *Cavalli et al.* [2006] observed aerosol over a boreal coniferous forest in southern Finland to lose marine character and to acquire chemical features resembling those of European continental sites, with a marked increase in the concentrations of all major anthropogenic aerosol constitutes as the arrival of northerly airflow progressively change the direction from west to east.

[17] However, the possibilities of emission due to forest burning was remote and natural emission of bio aerosol from the vegetation along with the photochemical oxidation of isoprene and its subsequent contribution to nucleation mode [*Claeys et al.*, 2004; *Buzorins et al.*, 2001] would contribute to the nucleation mode which ranged between 1.24–13.35 μgm^{-3}. Significant increase in nucleation mode (8.7% of the total aerosol mass) was observed over the mangrove forest during premonsoon (June). High concen-

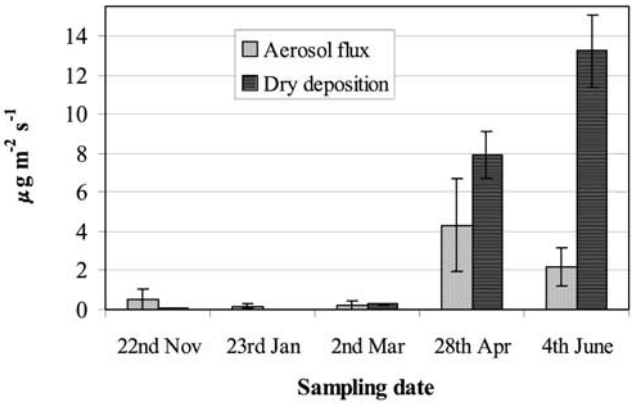

Figure 3. Datewise variation of the rate of aerosol flux (F) and dry deposition flux(F_d) (bars represent the overall uncertainties associated with the flux measurements).

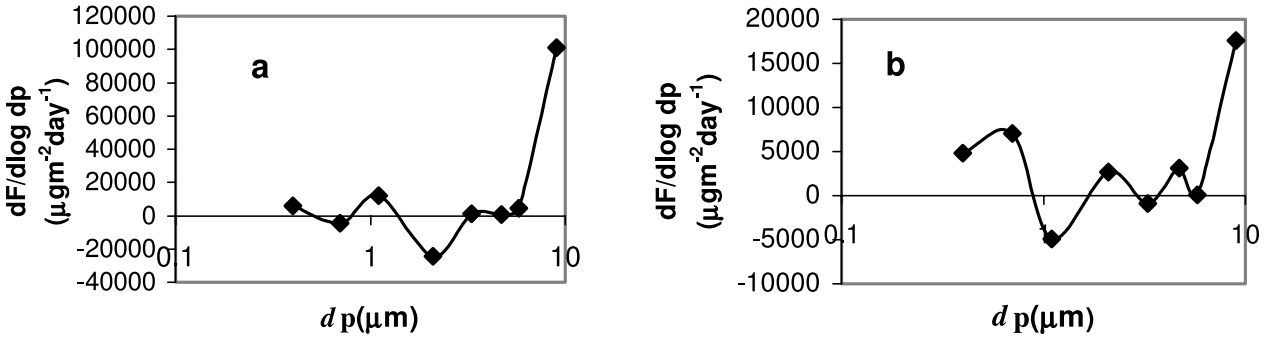

Figure 4. Change of rate of aerosol loading in different size mode for (a) November and (b) March.

tration in the coarse mode in general and, its enhanced contribution of 59.8 to 63.8% during premonsoon in particular indicates the impact by soil dust particle. *Dey et al.* [2004] observed the impact of dust loading on aerosol optical depth during the premonsoon season over the Indo-Gangetic basin. Air borne particles originated from biological activities of the microorganisms on leaf surfaces and forest litters to gather with wind blown pollen grains could contribute to the coarse fraction in the forest areas [*Artaxo et al.*, 1994]. Few biogenic elements (K, P, S, Zn, Rb) could also be released from the leaves to the atmosphere during guttation and transpiration [*Nemeruyk*, 1970]. Considerable contribution to coarse fraction from the wind blown secreted salt via salt gland of mangrove plants could also be specific for the Sundarban Mangrove forest in the NE coast of Bay of Bengal [*Popp*, 1984]. Increased temperature, wind velocity and relative humidity could enhance the natural emission and the biological activity during premonsoon time in the forested area. In order to determine the impact of sources other than the marine, ratios of dissolved ions with sodium were calculated assuming Na to be of the marine origin. The observed ratios along with their literature values [*Riley and Chester*, 1971] are given in Table 3. Ratio of ions with respect to Na^+ was found to be higher for NO_3^-, NO_2^-, PO_4^{3-}, SO_4^{2-}, K^+, Ca^{2+}, lower for Cl^- and closer for Mg^{2+} in comparison with those obtained for seawater. Lower ratio for Cl^- could be due to the fractionation of sea salt and the average percentage of Cl^- depletion was found to be 72.1 with higher Cl^- depletion rate from accumulation and nucleation mode (77.2–81.7%) compared to that of coarse mode (67.2%). Over wet and well-vegetated mangrove forest inversion of temperature is a common phenomenon. In summer, inversion of temperature was observed for a limited period of time in the night (2300–0400 LT) (30 March to 3 April 2005), while in winter it was observed almost through out day and night except for the period between 0100–0600 LT, (21–24 January 2005). This resulted more loss of chloride from the coarse and nucleation mode compared to accumulation mode in January (Cl/Na = 0.6023 ± 0.1798) and reverse trend was observed in April (Cl/Na = 0.644 ± 0.262) (Figure 5).

[18] *Zhuang et al.* [1999] observed the decrease of Cl^- depletion from 98% to 10% as particle size increases from 1.8 to18 μm. *Pakkanen* [1996] also observed similar size dependence in Finland. Smaller particles provide more surface area and their longer residence times could facilitate the reactions between gaseous HNO_3 and H_2SO_4 on the sea-salt particle surface. Coarse-mode nitrate is mainly formed by the reaction of HNO_3 with sea-salt particles, especially when maritime and urban air masses are mixed together. This reaction has been suggested to be the major path for the formation of coarse-mode nitrate at many coastal areas. NO_x transforms into gaseous nitrous and nitric acids, which later react with NaCl in sea-salt aerosols to form $NaNO_3$ and HCl in the chloride depletion reaction [*Kerminen et al.*, 1997]. NO_x concentration varied between 0.07 and 6.9 μg m^{-3} at this site during study period and played an important role for chloride depletion.

[19] The heterogeneous multiphase chemical reactions of OH radical, NO_3 radical, N_2O_5 (gas), $ClONO_2$ (gas) with aerosol chloride could also be the key process for the depletion of chloride from the aerosol in this coast [*Knipping and Dabdub*, 2003]. Ratios of NO_3^-, NO_2^- and NH_4^+ to Na^+ showed enrichment in the increasing order with decreasing size. Higher values of its ratio indicate the gas to

Table 3. Ratios of Different Ions With Respect to Sodium in Seawater and in Different Size Mode of Aerosol

Species	Coarse	Accumulation	Nucleation	Total	Sea
Cl/Na	0.59	0.33	0.41	0.50	1.8
NO_2/Na	0.0062	0.012	0.027	0.009	—
NO_3/Na	0.12	0.26	0.44	0.18	11.78×10^{-6}
PO_4/Na	0.53	0.59	0.6	0.55	2.17×10^{-6}
SO_4/Na	0.53	0.97	0.89	0.67	0.25
K/Na	0.16	0.091	0.074	0.135	0.037
NH_4/Na	0.0084	0.16	0.255	0.069	1.33×10^{-6}
Ca/Na	0.22	0.18	0.22	0.21	0.038
Mg/Na	0.07	0.846	0.082	0.076	0.12

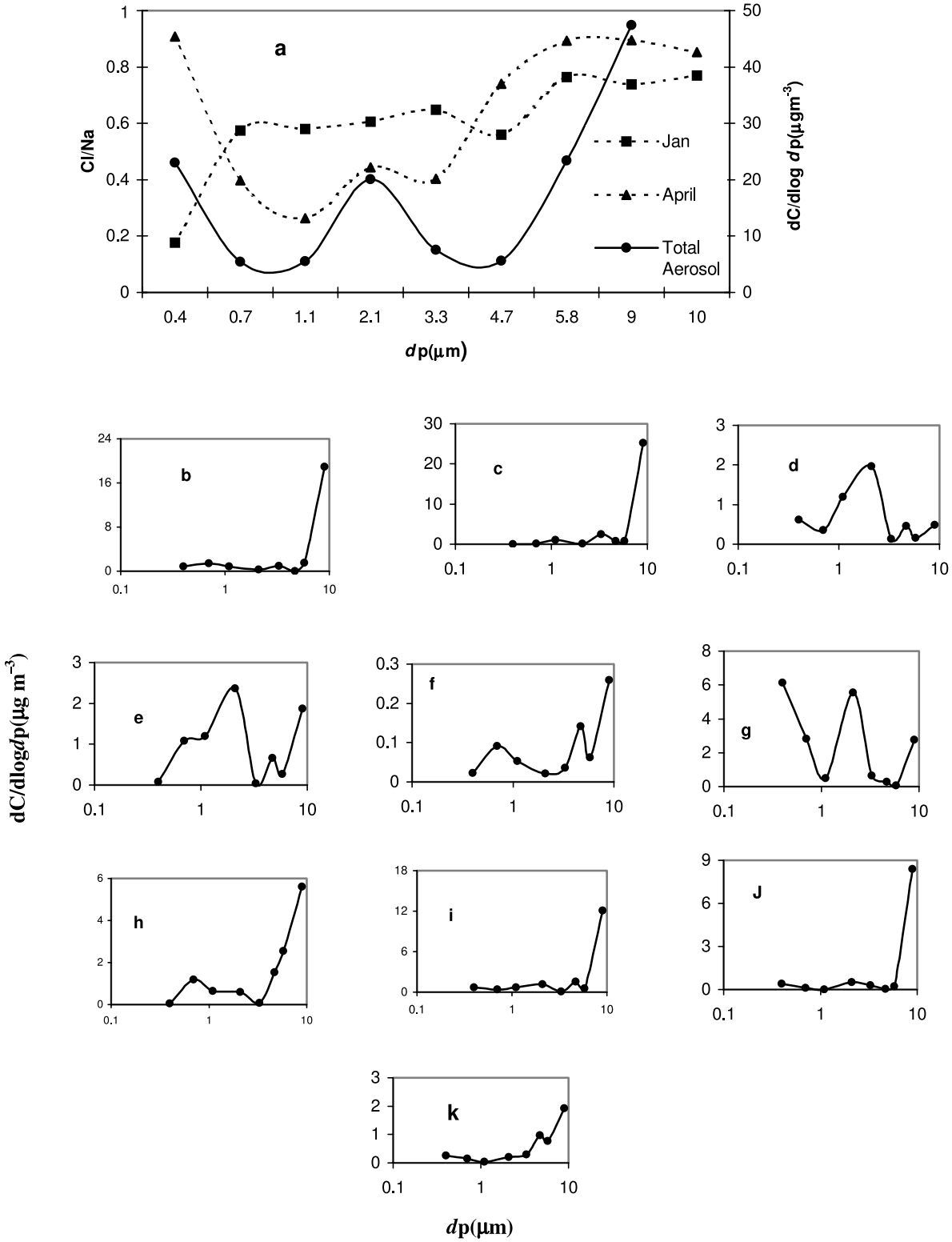

Figure 5. Size distribution of (a) total aerosol (average of five sets of data) and Cl/Na ratio (April and January), (b) Na^{+}, (c) Cl^{-}, (d) NH_4^{+}, (e) NO_3^{-}, (f) NO_2^{-}, (g) SO_4^{-2}, (h) PO_4^{-3}, (i) K^{+}, (j) Ca^{+2}, and (k) Mg^{+2} (average of five sets of data).

solid conversion of NH_3 to NH_4NO_3 in the accumulation and nucleation mode. Ammonia showed a decreasing concentration in the atmosphere from its maximum value of 16.58 μg m^{-3} in January to 3 μg m^{-3} in April.

[20] Concentrations of non-sea-salt sulphate were found to be 51.8, 74 and 72 percent of the total aerosol sulphate in the coarse, accumulation and nucleation mode, respectively. Sulphate shows prominent peak in accumulation and nu-

Table 4. VARIMAX-Rotated Factor-Loading Matrix for Aerosol

Variable	Factor 1	Factor 2	Factor 3	Factor 4	Factor 5	Communality
Na	0.94	−0.17	−0.08	0.2	−0.074	0.96
NH_4	0.64	0.64	−0.22	−0.21	0.03	0.91
K	0.26	0.25	0.83	−0.26	−0.19	0.93
Ca	0.74	−0.18	0.46	−0.22	0.08	0.84
Mg	0.81	−0.07	−0.5	0.12	0.02	0.93
Cl	0.76	−0.24	0.16	0.28	−0.46	0.96
NO_2	−0.12	0.7	0.15	0.65	0.05	0.95
NO_3	0.12	0.93	0.21	−0.05	0.02	0.92
PO_4	0.49	−0.35	0.52	0.23	0.51	0.95
SO_4	0.77	0.27	−0.41	−0.22	0.17	0.92
Eigenvalue	4.0	2.13	1.74	0.82	0.56	
Percent of Variation	40.1	21.3	17.4	8.2	5.6	

cleation mode. The sulphate concentration corresponding to the coarse mode may originate from marine source but occurrence of maximum percentage of non-sea-salt sulphate in the accumulation mode indicates their formation by the growth of the condensation mode particles and/or evaporation of large droplets formed by the oxidation of SO_2 to H_2SO_4 [*Pandis et al.*, 1992]. This is further corroborated by the highest depletion of chloride from the accumulation mode. SO_4^{-2}/Cl ratio is significantly higher compared to that of seawater. Blooming of phytoplankton occurring almost through out the year [*Biswas et al.*, 2004] and sulphate reduction occurring in anoxic condition of the sediment could result considerable emission of biogenic emission of sulphur gases, which ultimately converted to non-sea-salt sulphate in the aerosol. Chloride depletion (Cl_{loss} in μM) for particles < 2.0 μm showed a positive correlation (r = 0.54, t = 0.05) with non-sea-sulphate (nss in μM) : Cl_{loss} = 0.028 + 2.45 [nss].

[21] Mass size distribution of the total aerosol was trimodal as is evident by Figure 5a and Figures 5b, 5c, 5d, 5e, 5f, 5g, 5h, 5i, 5j, and 5k showed the characteristics of the mass size distribution of various ionic components. Similarity of size distribution of both sodium and chloride with prominent coarse-mode peak (Figures 5b and 5c) indicated their common marine source. For mean size distribution of NH_4^+ and NO_3^- (Figures 5d and 5e) accumulation mode was more prominent compared to other two modes. Accumulation mode nitrate could be formed from NOx after its gas phase conversion to HNO_3 followed by the reaction with NH_3 to form NH_4NO_3. Distribution of NO_3^- in coarse mode was the result of reaction of HNO_3 or N_2O_5 with preexisting particles. Size distribution of NO_3^- showed a hump at the 0.4–0.7 μm ranges similar to the peak observed in the same range for NO_2^- (Figure 5f), which could be due to the successive photochemical loss of NO_3^- or decomposition of NO_3^- to NO_2^- [*Millero*, 1996]. Figure 5g showed a trimodal distribution of sulphate. Excess sulphate concentration was calculated from the nss sulphate that was not associated with NH_4^+. Excess sulphate concentration along with NO_3^- and NO_2^- could account for only 22.28% of depletion of chloride (Table 2). The significance of the response of chloride loss (Cl_{loss} in μM) for particles > 2.0 μm was tested by multiple regression analysis. The dependent variable was Cl_{loss} and the independent variables were non-sea-sulphate (nss in μM) and nitrate (NO_3^- in μM). Statistical analysis revealed significant correlation between Cl_{loss} with independent variable tested [Cl_{loss} = 0.021 + 2.49 [nss] + 6.7 [NO_3], R^2 = 78.89, p = 0.028]. Linear terms nss and NO_3^- were positive and influenced chloride loss from sea-salt particles.

[22] Size distribution of phosphate showed two peaks (Figure 5h) at coarse and accumulation mode with an average concentration of 10.6 ± 4.61 μg m^{-3}. Coarse-mode fraction was found to be 61.6% of the total aerosol phosphate. *Artaxo et al.* [2001] reported nighttime plant emission of phosphorus, which was about 2–5 times higher than that of daytime in the Amazon forest with an average concentration of 70 ng m^{-3} in the coarse mode. It was suggested that the forest released P in the coarse mode only at nighttime to minimize the risk of P loss to the overall ecosystem, sharing this key nutrient with only the nearest neighbors.

[23] The mass size distribution of K^+, Ca^{2+}, Mg^{2+} (Figures 5i, 5j, and 5k), showed unimodal distribution like Na^+ and Cl^- reflecting their major marine source. However, a small peak at 1.1–2.1 μm range indicated transport of wind blown dust to this pristine environment.

[24] To separate different aerosol components, the absolute principal component analysis was done [*Hopke*, 1985] for the quantification of elemental source profile. The variability in the concentration of water-soluble ions was used in a factor analysis model to study the relationship between observed variables. Table 4 shows the VARIMAX rotated factor loading matrix. It shows the communalities of the factor analysis that express the percentage of each element variability that was explained by the factor model and gives the variance explained by each retained factor. Factor loading larger than approximately 0.3 are statistically significant [*Heidam*, 1982]. The first factor had high loading for Na^+, NH_4^+, Ca^{2+}, Mg^{2+}, Cl^-, PO_4^{3-} and SO_4^{2-} and represented marine salt particle. Association of phosphate with the salt particles as observed in factor analysis (factor 1) indicated that considerable proportion of aerosol phosphate in coarse mode had marine source and the concentration of phosphate phosphorous in the NE coast of Bay of Bengal was found higher (Table 1) compared to that of the open ocean. Higher phosphate concentration in the surf zone was due to the nutrient run off from the mangrove-dominated estuaries at the land ocean boundary condition of Sundarban Mangrove forest. The second factor was due to the biogenic source of ammonia as well as its atmospheric transport from the land. Its association with NO_2^- and NO_3^- could be due to photochemical oxidation. Third factor was loaded with K^+, Ca^{2+} and PO_4^{3-} and represented the soil dust particle and

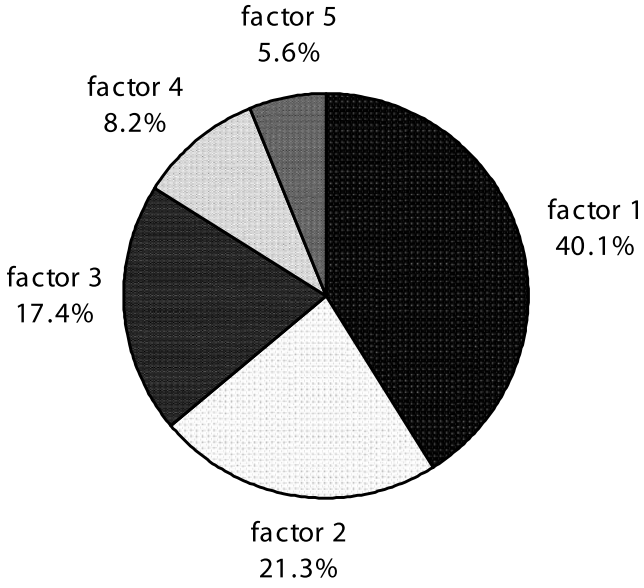

Figure 6. Total aerosol mass source apportionment.

factor 4 was associated with NO_2^- representing atmospheric transport of NOx from the adjacent metropolis. Higher concentration of phosphate in the aerosol over Sundarban Mangrove forest compared to other area with minimum anthropogenic influence [*Artaxo et al.*, 1990, 2001] could be due to the contribution from different sources as was evident by its association with factor 1, 3 and 5. Phosphate enters the atmosphere from a verity of sources such as continental-derived dust, sea spray and plant pollen [*Graham and Duce*, 1979; *Migon et al.*, 2001] and with increasing fluxes from anthropogenic sources, atmospheric input of phosphorus are believed to cause significant effects within coastal ecosystems [*Fang*, 2004]. One particular important issue evident in Table 2 was the presence of significant coarse-mode phosphorus concentration being higher than both nitrate and nss sulphate, and about the same concentration as total sulphate. *Artaxo et al.* [2002] showed higher concentration of coarse-mode phosphorus (pasture site = 37.9 ± 23.3 ng m^{-3}, forest site = 34.0 ± 23.7 ng m^{-3}) compared to that of sulphate (pasture = 24.0 ± 14.1, forest = 28.2 ± 15.9 nmol m^{-3}) in the aerosol in the wet season in Rondonia, Amazonia. Enhancement of coarse-mode phosphorus (46.9 ng m^{-3}) was also observed during dry season as a result of the long-range transport of biomass burning. *Dey et al.* [2004] showed strong seasonal variability in the Indo-Gangetic basin, with least spectral dependence of aerosol optical depth (AOD) during premonsoon, characterized by dust loading. The increased concentration of leachable inorganic phosphorus in the aerosol could be attributed by the dust particles. *Herut et al.* [1999] obtained 387 ± 205 μg seawater leachable phosphorus per g of dust collected at three sites along the Mediterranean coast of Israel.

[25] The five-factor model could explain 92.6% of the data variance and the first three components account for 78.8%. The communalities for all variables, in general are larger than 90%, indicating that the five factors could explain satisfactorily the observed elemental concentration. Figure 6 shows the total aerosol mass source apportionment. For the total aerosol samples, 40% of the aerosol mass was associated with marine aerosol, 26.9% with gas to solid converted particles, 17.4% with soil dust, 8.2% with NO_X transported by advective process, 5.6% with bio-aerosol component.

5. Conclusion

[26] The average atmospheric concentration of aerosol over Sundarban Mangrove forest at the NE coast of Bay of Bengal during Asiatic dry season was found to be 99.94 μg m^{-3}. The estimated rate of loading of aerosol ranged between 0.19 and 4.29 μg m^{-2} s^{-1} and dry deposition rate, between 0.019 and 13.21 μg m^{-2} s^{-1}. The aerosol distribution was trimodal with different in percentage contribution. Before the onset of monsoon, contribution of nucleation mode was found to increase from 2.81 to 8.7%. More loss of chloride from the coarse and nucleation mode was observed compared to accumulation mode in winter (Cl/Na = 0.6023 ± 0.1798) and reverse trend was observed in summer (Cl/Na = 0.644 ± 0.262). Significant correlation was obtained for chloride loss with non-sea-sulphate and nitrate for particles >2.0 μm. The aerosol composition appeared to have predominant urban influence as was evident by the presence of a nucleation mode, relatively high levels of sulphate and nitrate with high chloride depletion. The proximity of Calcutta and Haldia metropolis to the mangrove forest could influence on the forest air quality and depositional processes. The sum of water-soluble inorganic components accounted for 72.35% of the total aerosol mass with relatively higher contribution of phosphate. Occurrence of four types of particle: marine aerosol particle, naturally released biogenic particle, soil dust particle and particles derived from the anthropogenic and biogenic gases have been identified in the aerosol by factor analysis.

[27] **Acknowledgments.** Financial assistance from the Indian Space Research Organisation, Government of India, through the S. K. Mitra Center for Research in Space and Environment, University of Calcutta, and a fellowship to A.C. are gratefully acknowledged. Thanks are also due to Sundarban Biosphere Reserve and Divisional forest office, South 24 Parganas, Government of West Bengal, India, and Calcutta Port Trust, India, for permission to carry out the experiments. The authors appreciate the help extended by H. Biswas during manuscript revision.

References

APHA Intersociety Committee (1977). *Methods of Air Sampling and Analyses*, 2nd ed., edited by K. Moris, 511–513 pp., *Am. Publ. Health Assoc.*, Washington, D. C.

Artaxo, P., W. Maenhaut, H. Storms, and R. V. Grieken (1990), Aerosol characteristics and sources for the Amazon Basin during wet season, *J. Geophys. Res.*, *95*, 16,971–16,985.

Artaxo, P., F. Gerab, M. A. Yamasoe, and J. V. Martius (1994), Fine mode aerosol composition at three long-term atmospheric monitoring sites in the Amazon Basin, *J. Geophys. Res.*, *99*, 22,857–22,868.

Artaxo, P., E. T. Fernandes, J. V. Martius, M. A. Yamasoe, P. V. Hobbs, W. Maenhaut, K. M. Longo, and A. Castanho (1998), Large scale aerosol source apportionment in Amazonia, *J. Geophys. Res.*, *103*, 31,837–31,847.

Artaxo, P., M. O. Andreae, A. Guenther, and D. Rosenfeld (2001), Unveiling the lively atmosphere-biosphere interactions in the Amazon, *Global Change Newsl.*, *45*, 12–15.

Artaxo, P., J. V. Martin, M. A. Yamasoe, A. S. Procopio, T. M. Pauliquevis, M. O. Andreae, P. Guyon, V. L. Gatti, and A. M. C. Leal (2002), Physical and chemical properties of aerosols in the wet and dry seasons in Rondonia, Amazonia, *J. Geophys. Res.*, *107*(D20), 8081, doi:10.1029/2001JD000666.

Birmili, W., and A. Wiedensohler (2000), New particle formation in the continental boundary layer: Meteorological and gas phase parameter influence, *Geophys. Res. Lett.*, *27*, 3325–3328.

Biswas, H., S. K. Mukhopadhyay, T. K. De, S. Sen, and T. K. Jana (2004), Biogenic controls on the air-water carbon dioxide exchange in the Sundarban mangrove environment, northeast coast of Bay of Bengal, India, *Limnol. Oceanogr.*, *49*, 95–101.

Biswas, H., A. Chatterjee, S. K. Mukhopadhyay, T. K. De, S. Sen, and T. K. Jana (2005), Estimation of ammonia exchange at the land-ocean boundary condition of Sundarban mangrove, northeast coast of Bay of Bengal, India, *Atmos. Environ.*, *39*, 4489–4499.

Buzorins, G., U. Rannik, D. Nilsson, and M. Kulmala (2001), Vertical fluxes and micrometeorology during aerosol particle formation events, *Tellus, Ser. B*, *53*(4), 394–405.

Cavalli, F., M. C. Facchini, S. Decesari, L. Emblico, M. Mircea, N. R. Jensen, and S. Fuzzi (2006), Size segregated aerosol chemical composition at a boreal site in southern Finland, during the QUEST project, *Atmos. Chem. Phys.*, *6*, 993–1002.

Claeys, M., B. Graham, G. Vas, Wu Wang, R. Vermeylen, V. Pashynska, J. Cafmeyer, P. Guyon, M. O. Andreae, P. Artaxo, and W. Maenhaut (2004), Formation of secondary organic aerosols through photooxidation of isoprene, *Science*, *303*, 1173.

Clough, B. (1998), Mangrove forest productivity and biomass accumulation in Hinchinbrook Channel, Australia, *Mangroves Salt Marshes*, *2*, 191–198.

De Leeuw, G., F. P. Neele, M. Hill, M. H. Smith, and E. Vignati (2000), Production of sea spray aerosol in the surf zone, *J. Geophys. Res.*, *105*, 29,397–29,409.

Dey, S., S. N. Tripathi, R. P. Singh, and B. N. Holben (2004), Influence of dust storms on the aerosol optical properties over the Indo-Gangetic Basin, *J. Geophys. Res.*, *109*, D20211, doi:10.1029/2004JD004924.

Duce, R. A., and H. H. Woodcock (1971), Difference in chemical composition of atmospheric sea salt particles produced in the surf zone and on the open sea in Hawaii, *Tellus, Ser. A*, *23*, 427–434.

Fang, T. H. (2004), Phosphorus speciation and budget of the East China Sea, *Cont. Shelf Res.*, *24*, 1285–1299.

Ganguly, D., A. Jayaraman, and H. Gadhavi (2005), In situ ship cruise measurement of mass concentration and size distribution of aerosols over Bay of Bengal and their radiative impacts, *J. Geophys. Res.*, *110*, D06205, doi:10.1029/2004JD005325.

Gifford, F. A., and S. R. Hanna (1973), Modelling of urban air pollution, *Atmos. Environ.*, *7*, 131–136.

Graham, W. F., and R. A. Duce (1979), Atmospheric pathways of the phosphorus cycle, *Geochim. Cosmochim. Acta*, *43*, 1195–1208.

Grasshoff, K., et al. (Eds.) (1983), *Methods of Sea Water Analysis*, pp. 31–72, 125–187, Verlag Chemie, Weinheim.

Heidam, N. Z. (1982), Atmospheric aerosol factor models, mass and missing data, *Atmos. Environ.*, *16*, 1923–1931.

Herut, B., M. D. Krom, G. Pan, and R. Mortimer (1999), Atmospheric input of nitrogen and phosphorus to the southeast Mediterranean: Sources, fluxes and possible impact, *Limnol. Oceanogr.*, *44*(7), 1683–1692.

Hoffman, G. L., and R. A. Duce (1972), Consideration of the chemical fractionation of alkali and alkaline earth metals in the Hawaiian marine atmosphere, *J. Geophys. Res.*, *77*, 5161–5169.

Hopke, P. K. (1985), *Receptor Modeling in Environmental Chemistry*, John Wiley, Hoboken, N. J.

Hsu, S. A., and T. Whelan (1976), Transport of atmospheric sea salt in the coastal zone, *Environ. Sci. Technol.*, *10*, 281–283.

Jacobs, M. B., and S. Hochhieser (1958), Continuous sampling and ultra micro determination of nitrogen dioxide in air, *Anal. Chem.*, *30*(3), 426–428.

Jennerjahn, T. C., and V. Ittekkot (2002), Relevance of mangroves for the production and deposition of organic matter along tropical continental margins, *Naturwissenschaften*, *89*, 23–30.

Kerminen, V. M., T. A. Pakkanen, and R. E. Hillamo (1997), Interactions between inorganic trace gases and supermicrometer particles at a coastal site, *Atmos. Eniviron.*, *31*, 2753–2765.

Knipping, E. M., and D. Dabdub (2003), Impact of chlorine emission from sea-salt aerosol on coastal urban ozone, *Environ. Sci. Technol.*, *37*, 275–284.

Laaksonen, A., A. Hamed, J. Jouisensaari, L. Hilumen, F. Cavalli, W. Junkermann, A. Asmi, S. Fuzzi, and M. C. Facchini (2005), Cloud condensation nucleus production from nucleation events at a highly polluted region, *Geophys. Res. Lett.*, *32*, L06812, doi:10.1029/2004GL022092.

Lestari, P., A. K. Oskouie, and K. E. Noll (2003), Size distribution and dry deposition of particulate mass, sulphate and nitrate in an urban area, *Atmos. Environ.*, *37*, 2507–2516.

Lin, J., G. Fang, T. M. Holsen, and K. E. Noll (1993), A comparison of dry deposition modeled from size distribution data and measured with a smooth surface for total particle mass, lead, and calcium in Chicago, *Atmos. Environ., Part A*, *27*, 1131–1138.

McDonald, R. L., C. K. Unni, and R. A. Duce (1982), Estimation of atmospheric sea salt dry deposition: Wind speed and particle size dependence, *J. Geophys. Res.*, *87*, 1246–1250.

Migon, C., V. Sandroni, and J. P. Bethoux (2001), Atmospheric input of anthropogenic phosphorus to the northwest Mediterranean under oligotrophic conditions, *Mar. Environ. Res.*, *52*, 413–426.

Millero, J. F. (1996), *Chemical Oceanography*, 2nd ed., pp. 359–374, CRC Press, Boca Raton, Fla.

Mukhopadhyay, S. K., H. Biswas, T. K. De, B. K. Sen, S. Sen, and T. K. Jana (2002), Impact of Sundarban mangrove biosphere on the carbon dioxide and methane mixing ratios at the NE Coast of Bay of Bengal, India, *Atmos. Environ.*, *36*, 629–638.

Nemeruyk, G. E. (1970), Migration of salts into the atmosphere during transpiration, *Sov. Plant. Physiol.*, *17*, 560–566.

O'Dowd, C. D., M. Geever, M. K. Hill, S. G. Jennings, and M. H. Smith (1998), New particle formation: Spatial scales and nucleation rates in the coastal environment, *Geophys. Res. Lett.*, *25*, 1661–1664.

Pakkanen, T. A. (1996), Study of the formation of coarse particle nitrate aerosol, *Atmos. Environ.*, *30*, 2475–2482.

Pal Arya, S. (2001), *Introduction to Micrometeorology*, Elsevier, New York.

Pandis, S. N., J. H. Seinfeld, and C. Pilinis (1992), Heterogeneous sulphate production in an urban fog, *Atmos. Environ., Part A*, *26*, 2509–2522.

Parameswaran, K., P. R. Nair, R. Rajan, and M. V. Ramanna (1999), Aerosol loading in coastal and marine environment in INDOEX during winter season, *Curr. Sci.*, *76*(7), 947–955.

Pasquill, F., and F. B. Smith (1983), *Atmospheric Diffusion*, 3rd ed., pp. 309–358, Halsted, New York.

Petelski, T., and M. Chomka (2000), Sea salt emission from the coastal zone, *Oceanologia*, *42*, 399–410.

Popp, M. (1984), Chemical composition of Australian mangroves, inorganic ions and organic acids, *Z. Pflanzen Physiol.*, *113*, 411–421.

Pueschel, R. F. (1995), Atmospheric Aerosols, in *Composition Chemistry and Climate of the Atmosphere*, edited by H. B. Singh, 141 pp., Van Nostrand Reinhold, Hoboken, N. J.

Putaud, J. P., et al. (2000), Chemical mass closure and assessment of the origin of the submicron aerosol in the marine boundary layer and the free troposphere at Tenerife during ACE-2, *Tellus, Ser. B*, *52*, 141–168.

Raes, F., J. Wilson, J. P. Putaud, J. H. Seinfeld, P. Adams, R. Van Dingenen, and E. Vignati (2000), Formation and cycling of aerosols in the global troposphere, *Atmos. Environ.*, *34*, 4215–4240.

Rajeev, K., S. K. Nair, K. Parameswaran, and C. Suresh Raju (2004), Satellite observations of the regional distribution and transport over the Arabian Sea, Bay of Bengal and Indian Ocean, *Indian J. Mar. Sci.*, *33*(1), 11–29.

Riley, J. P., and R. Chester (1971), *Introduction to Marine Chemistry*, pp. 64–67, Elsevier, New York.

Sehmel, G. A., and W. H. Hodgson (1978), *A Model for Predicting Dry Deposition of Particles and Gases to Environmental Surfaces*, *PNL-SA-6721* (and in revised form October 1979, PNL-SA-6721-REV-1), Battelle, Pacific Northwest Lab., Richland, Wash.

Williamson, S. J. (1973), *Fundamentals of Air Pollution*, Addison-Wesley, Boston, Mass.

Zhuang, H., C. K. Chan, M. Fang, and A. S. Waxler (1999), Formation of nitrate and non-sea salt sulphate on coarse particles, *Atmos. Environ.*, *33*, 4223–4233.

N. Biswas and K. Ghosh, Glass Physics Section, Central Glass and Ceramic Research Institute, Jadavpur, Calcutta-32, India.

A. Chatterjee, C. Dutta, and S. Sen, Department of Chemistry, Calcutta University, 92 A.P.C. Road, Calcutta-700009, India.

D. Ganguly and T. K. Jana, Department of Marine Science, Calcutta University, 35 B.C. Road, Calcutta-700019, India. (tkjana@hotmail.com)